

Fig. 1. Flow cytometric analysis of the interaction of claudins (CLs) with the CF750-labeled C-terminal fragment of *Clostridium perfringens* enterotoxin (C-CPE). Mouse fibroblast L cells were incubated with 10 µg/ml CF750-labeled C-CPE or a mutant form of C-CPE (also labeled with CF750) for 1 h and then subjected to fluorescence-activated cell sorter analysis as described in the Materials and Methods. Unfilled curves show the results obtained when cells were not treated with C-CPE proteins. Filled curves show data from C-CPE-treated cells. FL1-H indicates fluorescent intensity and M1 indicates C-CPE-bound cells.

(Michl et al., 2001; Santin et al., 2005). Moreover, the C-terminal fragment of CPE (C-CPE) is a ligand of CL-3 and CL-4 (Sonoda et al., 1999). We previously prepared a CL-targeting cytotoxic molecule via fusion of C-CPE and a protein synthesis inhibitory factor (PSIF) derived from *Pseudomonas* exotoxin (Ebihara et al., 2006). We found that intratumoral or intravenous administration of C-CPE-fused PSIF attenuated the growth of murine breast cancer cells (Saeki et al., 2009, 2010). Thus, drugs that include all or part of CPE may be useful for targeting CLs in cancer therapy.

CLs are expressed throughout the body. Evaluation of the possible adverse effects of CL-targeting molecules is critical if the CPE technology described above is to be used for cancer therapy. However, no such hazard assessment has been performed to date. Here,

we investigated the tissue distribution of C-CPE and the tissue injury caused by C-CPE-fused PSIF.

2. Materials and methods

2.1. Cell cultures

Mouse fibroblast L cells expressing mouse CL-1, CL-2, CL-3, CL-4, or CL-5 were kindly provided by Dr. S. Tsukita (Kyoto University). Cells were cultured in Eagle's minimum essential medium with 10% (v/v) fetal calf serum and 500 µg/ml G418 at 37 °C under a 5% (v/v) CO₂ atmosphere.

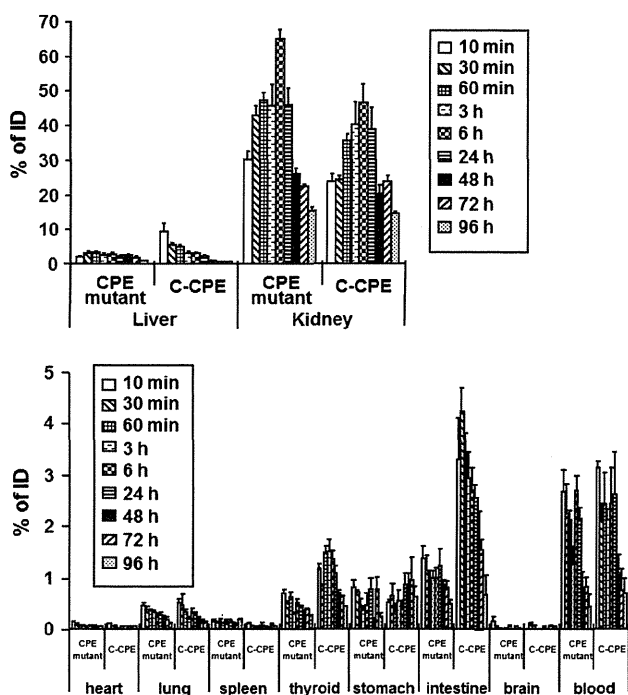


Fig. 2. *In vivo* distribution of the CF750-labeled C-terminal fragment of *Clostridium perfringens* enterotoxin (C-CPE). Mice were intravenously injected with 2 µg/mouse CF750-labeled C-CPE or a CF750-labeled C-CPE mutant. Tissues were removed at the indicated times after injection and the intensity of fluorescence of each tissue was measured as described in the Materials and Methods. Tissue C-CPE levels were calculated as percentages of injected doses. Data are means ± SEM (*n* = 5). ID, injected dose.

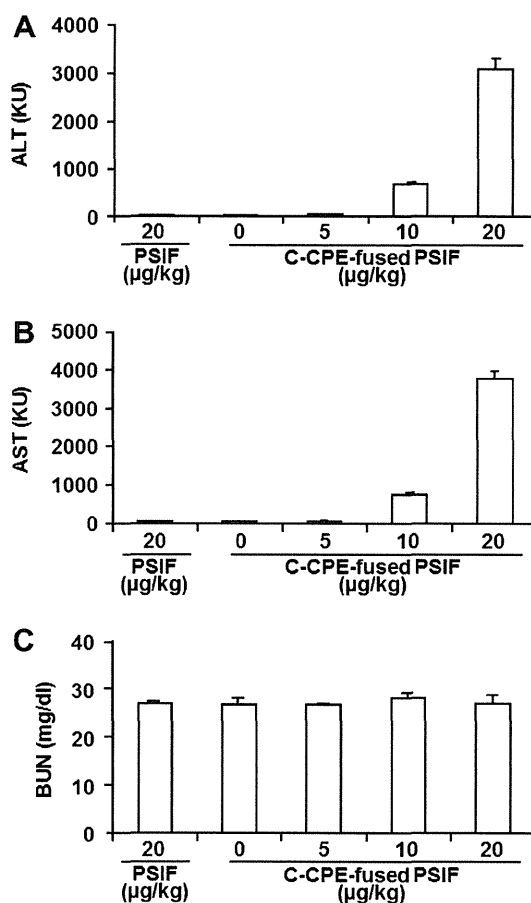


Fig. 3. Serum markers of liver and kidney injury in mice injected with protein synthesis inhibitory factor (PSIF) fused to the C-terminal fragment of *Clostridium perfringens* enterotoxin (C-CPE). Mice were intravenously injected with PSIF at 2 µg/kg or C-CPE-fused PSIF at 0, 5, 10, or 20 µg/kg. Twenty-four hours later, serum ALT (A), AST (B), and BUN (C) levels were measured as described in the Materials and Methods. Data are presented as means ± SEM (*n* = 5).

2.2. Preparation of C-CPE and C-CPE mutant protein

C-CPE, and a mutant form thereof, in which Ala was substituted with Tyr and Leu at positions 306 and 315, were prepared as described previously (Takahashi et al., 2008). Briefly, recombinant plasmids derived from pET-16b, pET-C-CPE encoding histidine (His)-tagged C-CPE, or a pET-C-CPE mutant encoding His-tagged C-CPE mutant protein, were transduced into *Escherichia coli* strain BL21 (DE3) (Novagen, Darmstadt, Germany), and production of recombinant proteins was induced by adding isopropyl-β-D-thiogalactopyranoside. Harvested cells were lysed in buffer A (10 mM Tris-HCl [pH 8.0], 400 mM NaCl, 5 mM MgCl₂, 0.1 mM phenylmethylsulfonyl fluoride, 1 mM 2-mercaptoethanol, and 10% [v/v] glycerol). Each lysate was applied to a HiTrap chelating HP column (GE Healthcare, Chalfont St Giles, Buckinghamshire, UK), and the recombinant protein was eluted with buffer A containing imidazole. This buffer was exchanged for phosphate-buffered saline (PBS) by using a PD-10 column (GE Healthcare), and the purified proteins dissolved in PBS were stored at -80 °C until use. The purity of the recombinant proteins was confirmed by sodium dodecyl sulfate-polyacrylamide gel electrophoresis followed by staining with Coomassie brilliant blue. Protein concentrations were quantified with a BCA protein assay kit, using bovine serum albumin (BSA) as a standard (Pierce Chemicals, Rockford, IL).

2.3. Animals

Female BALB/c mice (6–8 weeks of age) were purchased from SLC, Inc. (Shizuoka, Japan). Mice were housed at 23 ± 1.5 °C with a 12-h light/12-h dark cycle and had free access to water and commercial chow (Type MF; Oriental Yeast, Tokyo, Japan). Mice were allowed to adapt to these conditions for at least 1 week after arrival. All animal experiments adhered to the ethical guidelines of the Graduate School of Pharmaceutical Sciences, Osaka University.

2.4. Preparation of CF750-labeled C-CPE proteins

C-CPE and the mutant form of the protein were labeled with the fluorescent dye CF750 by using a Xenolight CF750 rapid antibody-labeling kit (Caliper Life Sciences, Inc., Hopkinton, MA), in accordance with the manufacturer's instructions. The concentrations of labeled C-CPEs were calculated according to the manufacturer's protocol by using the following equation: Concentration (mg/ml) = [(absorbance at 280 nm minus (absorbance at 755 nm × 0.3))/0.46] × dilution factor.

2.5. Fluorescence-activated cell sorter (FACS) analysis

L-cells expressing various CLs were harvested with trypsin and suspended in PBS. The cells were incubated with C-CPE or the mutant form of C-CPE for 1 h at 4 °C; this was followed by incubation with anti-His-tag antibody. Cells were next incubated with fluorescein-labeled secondary antibody, and cells that bound the test proteins were detected and analyzed by flow cytometry (FACScalibur, Becton Dickinson, Franklin Lakes, NJ).

2.6. Tissue distribution of injected proteins

C-CPE, or the mutant form thereof, labeled with CF750, was intravenously injected into mice at 2 µg/100 µl of PBS per mouse. Mice were sacrificed 10 min, 30 min, 60 min, 3 h, 6 h, 24 h, 48 h,

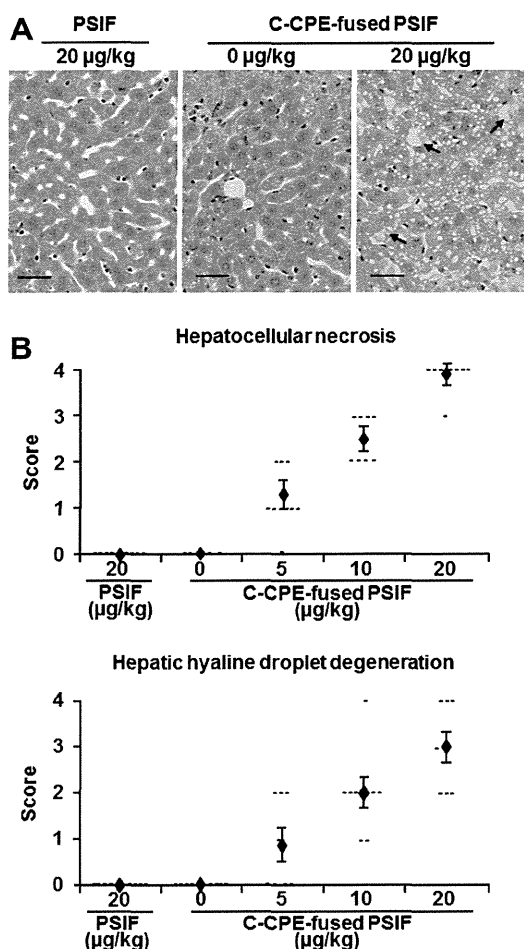


Fig. 4. Histological analysis of the livers of mice injected with protein synthesis inhibitory factor (PSIF) fused to the C-terminal fragment of *Clostridium perfringens* enterotoxin (C-CPE). Mice were intravenously injected with PSIF at 20 µg/kg or C-CPE-fused PSIF at 0, 5, 10, or 20 µg/kg (n = 7 or 8). Twenty-four hours later, the livers were removed and fixed in formaldehyde. Sections were stained with hematoxylin–eosin and examined microscopically for pathology. A representative micrograph is shown in panel A; arrows indicate regions of injury (scale bar, 60 µm). The extents of hepatocellular necrosis and hepatic hyaline droplet degeneration were scored (panel B) as follows: 0, none; 1, very mild; 2, mild; 3, moderate; or 4, high. Each horizontal dash represents the score of one sample. Data are means ± SEM (n = 7 or 8).

72 h, or 96 h later. The blood, heart, lung, liver, spleen, kidney, thyroid, stomach, intestine, and brain were excised from each mouse. The blood and organs from each mouse were placed side-by-side and imaged by using a Maestro EX *in vivo* imaging system, version 2.10.0 (Cambridge Research & Instrumentation Inc., Woburn, MA). The imaging system was equipped with an excitation filter (wavelength 229–684 nm). Fluorescence was detected by a CCD camera equipped with a C-mount lens and a long-pass emission filter (745 nm). Spectral data “cubes” were created by acquisition of a series of images obtained by using different wavelengths. In such cubes, each pixel is associated with a spectrum. Maestro software can be used to analyze these data; any autofluorescence can be identified, separated from the CF750 fluorescence, and removed. The resulting signals (counts) from each tissue were used to evaluate C-CPE distributions. The levels of C-CPEs in each tissue, as percentages of injected doses, were calculated. Total blood volume was calculated as 8% of body weight.

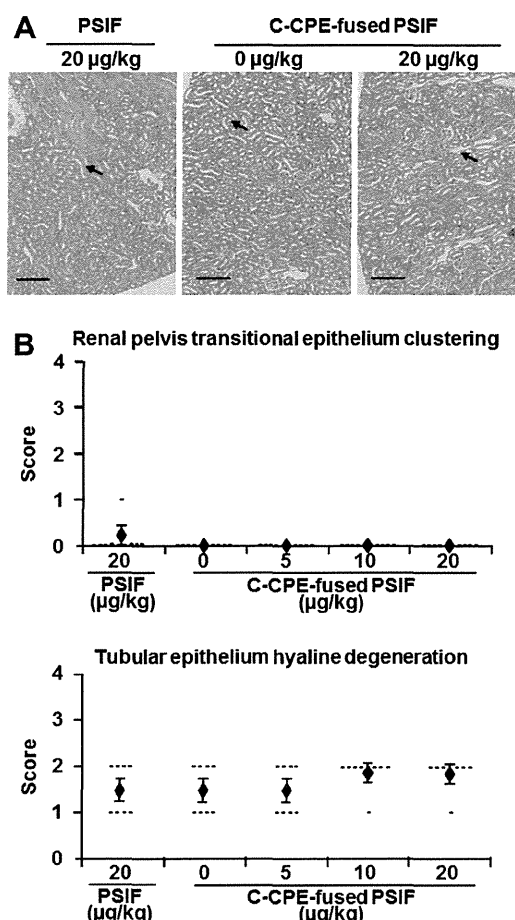


Fig. 5. Histological analysis of the kidneys of mice injected with protein synthesis inhibitory factor (PSIF) fused to the C-terminal fragment of *Clostridium perfringens* enterotoxin (C-CPE). Mice were intravenously injected with PSIF at 20 µg/kg or C-CPE-fused PSIF at 0, 5, 10, or 20 µg/kg (n = 7 or 8). Twenty-four hours later, the kidneys were removed and fixed in formaldehyde. Sections were stained with hematoxylin–eosin and examined microscopically for pathology. A representative micrograph is shown in panel A; arrows indicate regions of injury (scale bar, 240 µm). The extent of clustering of the renal pelvis transitional epithelium and the level of hyaline degeneration of the tubular epithelium were scored (panel B) as follows: 0, none; 1, very mild; 2, mild; 3, moderate; or 4, high. Each horizontal dash represents the score of one sample. Data are means ± SEM (n = 7 or 8).

2.7. Preparation of C-CPE-fused PSIF

PSIF and C-CPE-fused PSIF were prepared as described previously (Saeki et al., 2009). In brief, plasmid pET-PSIF or pET-C-CPE-PSIF was transduced into *E. coli* BL21 (DE3) and recombinant protein production was induced by adding 0.25 mM isopropyl-β-D-thiogalactopyranoside. Harvested cells were lysed in buffer A. The lysates were centrifuged and the supernatants applied to Hi-Trap chelating HP columns. Recombinant proteins were eluted with imidazole-containing buffer A. This buffer was exchanged for PBS by using a PD-10 column, and the purified protein solutions were stored at –80 °C until use. Protein concentrations were quantified with a BCA protein assay kit, using BSA as a standard.

2.8. Biochemical assays

Mice were intravenously injected with 100 µl of C-CPE-fused PSIF at 0, 5, 10, or 20 µg/kg, or with 100 µl of PSIF at 20 µg/kg.

Twenty-four hours after the injection, serum levels of alanine aminotransferase (ALT), aspartate aminotransferase (AST), and blood urea nitrogen (BUN) were measured with commercial kits (Transaminase-CII kit [ALT, AST] and Blood Urea Nitrogen-B Test [BUN]; Wako Pure Chemicals, Osaka, Japan).

2.9. Histological analysis

Livers and kidneys were removed and fixed in 4% (v/v) paraformaldehyde. Thin sections were stained with hematoxylin and eosin before histological observation. The extent of injury was scored as 0, none; 1, very mild; 2, mild; 3, moderate; or 4, high.

3. Results

3.1. Tissue distribution of the CL-3/-4-binding agent C-CPE

The fluorescent dye CF750 was conjugated to the CL-3/-4-binding agent C-CPE to allow the tissue distribution of C-CPE to be monitored. FACS analysis revealed that CF750-labeled C-CPE bound to CL-3- or CL-4-expressing L-cells but not to mock-, CL-1-, CL-2-, or CL-5-expressing L cells (Fig. 1). Thus, labeling of C-CPE with CF750 did not affect the binding profile of C-CPE to CLs. As a control, we also prepared a CF750-labeled C-CPE mutant protein lacking CL-binding activity; Ala was substituted for the wild-type Tyr306 and Leu315 in the mutant protein (Takahashi et al., 2008). The C-CPE mutant did not bind to the cells (Fig. 1).

C-CPE was evident in the kidney (24.0% of the injected dose), liver (9.5%), intestine (3.3%), and thyroid (1.2%) 10 min after intravenous injection (Fig. 2). The levels of C-CPE in the liver, intestine, and thyroid gradually fell thereafter, to 0.4%, 0.7%, and 0.4% of the injected dose, respectively, at 96 h post-injection. In contrast, the level of C-CPE in the kidney increased to 46.5% of the injected dose 6 h after injection and only then began to fall, reaching 14.4% of the injected dose 96 h post-injection. The control C-CPE mutant protein became distributed in the liver (2.0% of the injected dose), intestine (1.4%), and thyroid (0.7%) at levels much lower than those of C-CPE at 10 min post-injection, but the levels of the mutant protein in the kidney were comparable to those of C-CPE (Fig. 2). Therefore, the liver may be a major target tissue of CL-3/-4-binding protein, whereas accumulation in the kidney may not be associated with CL-3/-4 targeting.

3.2. Effects of a CL-3/-4-targeting toxin on the liver and kidney

We previously found that tail vein injection of C-CPE-fused PSIF at 5 µg/kg every 2 days for 14 days had anti-tumor activity without hepatotoxicity or nephrotoxicity (Saeki et al., 2010). Here, to evaluate the acute toxicity of a CL-targeting toxin to the liver and kidney, we intravenously injected mice with C-CPE-fused PSIF, or control PSIF alone, and measured biochemical markers of liver (ALT and AST) and kidney (BUN) injury 24-h later. Injection of PSIF alone (20 µg/kg) did not increase serum ALT, AST, or BUN levels. Injection of C-CPE-fused PSIF at doses of 0, 5, 10, and 20 µg/kg increased serum ALT and AST levels in a dose-dependent manner (ALT: 21, 49, 668, and 3053 karmen unit (KU) respectively; AST: 49, 68, 764, and 3781 KU, respectively) (Fig. 3A and B). In contrast, injection of C-CPE-fused PSIF, even at 20 µg/kg, did not increase the serum BUN level (Fig. 3C). Injection of C-CPE-fused PSIF at 10 or 20 µg/kg, but not at 5 µg/kg, caused body weight loss and reduced mobility (data not shown). Histologically, C-CPE-fused PSIF caused hepatocellular necrosis and hyaline droplet degeneration (Fig. 4A, B). Although injection of C-CPE-fused PSIF caused slight hyaline degeneration of the tubular epithelium of the kidney, injection of PSIF alone had a similar effect (Fig. 5A and B). Therefore, the low-level

kidney injury evident after administration of C-CPE-fused PSIF may not have been associated with the targeting of CLs.

4. Discussion

CPE was the first CL-3/-4-targeting toxin to be described (Fujita et al., 2000; Sonoda et al., 1999), and C-CPE-fused PSIF was the second (Ebihara et al., 2006; Saeki et al., 2009). A series of studies using CPE and C-CPE have provided proof-of-concept that CL targeting is a strategy for cancer therapy (Long et al., 2001; Michl et al., 2001; Neesse et al., 2013; Saeki et al., 2009, 2010; Santin et al., 2005). However, because CL-3 and CL-4 are expressed in various normal tissues (Morita et al., 1999; Turksen and Troy, 2011), risk assessment of CL-targeting molecules is needed when CPE technology is applied to cancer therapy. Here, we found that systemic injection of a C-CPE-fused toxin resulted in acute hepatic, but not renal, toxicity 24 h after injection in mice.

After injection, C-CPE accumulates to the greatest extent in the liver and kidney. The expression profiles of CL-3 and CL-4 differ in these two tissues. In the liver, CL-3 is locally expressed in the lateral membranes of all lobular hepatocytes (Rahner et al., 2001); the liver does not express CL-4 (Morita et al., 1999). In contrast, CL-3 and CL-4 are locally expressed, in the kidney, in the lateral membranes of epithelial-cell sheets of the loop of Henle, the distal tubule, and the collecting duct (Balkovetz, 2009). Epithelial cells of the kidney form a boundary between the inner and outer regions, and the TJs act as barriers, preventing free movement of solutes across epithelial sheets (Hou et al., 2010; Milatz et al., 2010). In contrast, hepatocytes do not have a barrier function, with the exception of those located in the canaliculi. Therefore, CL-targeting molecules can access CL-3 in parts of the liver other than the canaliculi, but not CL-3 and CL-4 in the renal epithelium. C-CPE-fused PSIF must be taken up by cells if the drug is to be cytotoxic, because inhibition of ribosomal elongation factor-2 by the PSIF domain is the cause of cell death (Ebihara et al., 2006; Kreitman and Pastan, 2006; Ogata et al., 1990).

Here, we found that hepatic accumulation of a toxin fused to C-CPE could have adverse effects if C-CPE-based cancer therapy were prescribed. C-CPE binds to both CL-3 and CL-4. Levels of CL-4 are increased more frequently than those of CL-3 in cancers such as breast, gastric, intestinal, ovarian, pancreatic, and prostate carcinomas (Singh et al., 2010; Tsukita et al., 2008; Turksen and Troy, 2011). Thus, development of a C-CPE mutant that binds to CL-4 but not to CL-3 may be useful in cancer therapy. We previously found that modulation of the electrostatic profile of the C-CPE surface can change the CL-binding profile (Takahashi et al., 2012). Veshnyakova et al. (2012) showed that the C-CPE residues, Leu223, Asp225, and Arg227, were involved in binding to CL-3, whereas Leu254, Ser256, Ile258, and Asp284 were involved in binding to CL-4. Manipulation of the electrostatic surface and the C-CPE residues may allow us to develop a C-CPE mutant that binds specifically to CL-4.

Acknowledgements

We thank the staff of our laboratory for their useful comments and discussion. This work was supported by Grants-in-Aids for Scientific Research from the Ministry of Education, Culture, Sports, Science, and Technology of Japan (Nos. 21689006 and 24390042); by a Health and Labor Sciences Research Grant from the Ministry of Health, Labour, and Welfare of Japan; by the Takeda Science Foundation; by the Nakatomi Foundation; and by the Platform for Drug Discovery, Informatics, and Structural Life Science of the Ministry of Education, Culture, Sports, Science, and Technology, Japan.

References

Adair, J.R., Howard, P.W., Hartley, J.A., Williams, D.G., Chester, K.A., 2012. Antibody-drug conjugates – a perfect synergy. *Expert. Opin. Biol. Ther.* 12, 1191–1206.

Anderson, J.M., Van Itallie, C.M., 2009. Physiology and function of the tight junction. *Cold Spring Harbor Perspect. Biol.* 1, a002584.

Balkovetz, D.F., 2009. Tight junction claudins and the kidney in sickness and in health. *Biochim. Biophys. Acta* 1788, 858–863.

Dent, S., Oyan, B., Honig, A., Mano, M., Howell, S., 2013. HER2-targeted therapy in breast cancer: a systematic review of neoadjuvant trials. *Cancer Treat. Rev.* 39, 622–631.

Ebihara, C., Kondoh, M., Hasuike, N., Harada, M., Mizuguchi, H., Horiguchi, Y., Fujii, M., Watanabe, Y., 2006. Preparation of a claudin-targeting molecule using a C-terminal fragment of *Clostridium perfringens* enterotoxin. *J. Pharmacol. Exp. Ther.* 316, 255–260.

Farquhar, M.G., Palade, G.E., 1963. Junctional complexes in various epithelia. *J. Cell Biol.* 17, 375–412.

Fujita, K., Katahira, J., Horiguchi, Y., Sonoda, N., Furuse, M., Tsukita, S., 2000. *Clostridium perfringens* enterotoxin binds to the second extracellular loop of claudin-3, a tight junction integral membrane protein. *FEBS Lett.* 476, 258–261.

Furuse, M., Tsukita, S., 2006. Claudins in occluding junctions of humans and flies. *Trends Cell Biol.* 16, 181–188.

Hou, J., Renigunta, A., Yang, J., Waldegger, S., 2010. Claudin-4 forms paracellular chloride channel in the kidney and requires claudin-8 for tight junction localization. *Proc. Natl. Acad. Sci. USA* 107, 18010–18015.

Jemal, A., Siegel, R., Ward, E., Hao, Y., Xu, J., Murray, T., Thun, M.J., 2008. Cancer statistics, 2008. *CA Cancer J. Clin.* 58, 71–96.

Kreitman, R.J., Pastan, I., 2006. Immunotoxins in the treatment of hematologic malignancies. *Curr. Drug Targets* 7, 1301–1311.

Long, H., Crean, C.D., Lee, W.H., Cummings, O.W., Gabig, T.G., 2001. Expression of *Clostridium perfringens* enterotoxin receptors claudin-3 and claudin-4 in prostate cancer epithelium. *Cancer Res.* 61, 7878–7881.

McClane, B.A., Chakrabarti, G., 2004. New insights into the cytotoxic mechanisms of *Clostridium perfringens* enterotoxin. *Anaerobe* 10, 107–114.

Michl, P., Buchholz, M., Rolke, M., Kunsch, S., Lohr, M., McClane, B., Tsukita, S., Leder, G., Adler, G., Gress, T.M., 2001. Claudin-4: a new target for pancreatic cancer treatment using *Clostridium perfringens* enterotoxin. *Gastroenterology* 121, 678–684.

Milatz, S., Krug, S.M., Rosenthal, R., Gunzel, D., Muller, D., Schulzke, J.D., Amasheh, S., Fromm, M., 2010. Claudin-3 acts as a sealing component of the tight junction for ions of either charge and uncharged solutes. *Biochim. Biophys. Acta* 1798, 2048–2057.

Mineta, K., Yamamoto, Y., Yamazaki, Y., Tanaka, H., Tada, Y., Saito, K., Tamura, A., Igarashi, M., Endo, T., Takeuchi, K., Tsukita, S., 2011. Predicted expansion of the claudin multigene family. *FEBS Lett.* 585, 606–612.

Morita, K., Furuse, M., Fujimoto, K., Tsukita, S., 1999. Claudin multigene family encoding four-transmembrane domain protein components of tight junction strands. *Proc. Natl. Acad. Sci. USA* 96, 511–516.

Neesse, A., Hahnenkamp, A., Griesmann, H., Buchholz, M., Hahn, S.A., Maghnoou, A., Fendrich, V., Ring, J., Sipos, B., Tuveson, D.A., Bremer, C., Gress, T.M., Michl, P., 2013. Claudin-4-targeted optical imaging detects pancreatic cancer and its precursor lesions. *Gut* 62, 1034–1043.

Ogata, M., Chaudhary, V.K., Pastan, I., FitzGerald, D.J., 1990. Processing of *Pseudomonas* exotoxin by a cellular protease results in the generation of a

37,000-Da toxin fragment that is translocated to the cytosol. *J. Biol. Chem.* 265, 20678–20685.

Rahner, C., Mitic, L.L., Anderson, J.M., 2001. Heterogeneity in expression and subcellular localization of claudins 2, 3, 4, and 5 in the rat liver, pancreas, and gut. *Gastroenterology* 120, 411–422.

Rodriguez-Boulan, E., Nelson, W.J., 1989. Morphogenesis of the polarized epithelial cell phenotype. *Science* 245, 718–725.

Saeki, R., Kondoh, M., Kakutani, H., Tsunoda, S., Mochizuki, Y., Hamakubo, T., Tsutsumi, Y., Horiguchi, Y., Yagi, K., 2009. A novel tumor-targeted therapy using a claudin-4-targeting molecule. *Mol. Pharmacol.* 76, 918–926.

Saeki, R., Kondoh, M., Kakutani, H., Matsuhisa, K., Takahashi, A., Suzuki, H., Kakamu, Y., Watari, A., Yagi, K., 2010. A claudin-targeting molecule as an inhibitor of tumor metastasis. *J. Pharmacol. Exp. Ther.* 334, 576–582.

Santin, A.D., Cane, S., Bellone, S., Palmieri, M., Siegel, E.R., Thomas, M., Roman, J.J., Burnett, A., Cannon, M.J., Pecorelli, S., 2005. Treatment of chemotherapy-resistant human ovarian cancer xenografts in C.B-17/SCID mice by intraperitoneal administration of *Clostridium perfringens* enterotoxin. *Cancer Res.* 65, 4334–4342.

Singh, A.B., Sharma, A., Dhawan, P., 2010. Claudin family of proteins and cancer: an overview. *J. Oncol.* 2010, 541957.

Sonoda, N., Furuse, M., Sasaki, H., Yonemura, S., Katahira, J., Horiguchi, Y., Tsukita, S., 1999. *Clostridium perfringens* enterotoxin fragment removes specific claudins from tight junction strands: evidence for direct involvement of claudins in tight junction barrier. *J. Cell Biol.* 147, 195–204.

Stahelin, L.A., 1973. Further observations on the fine structure of freeze-cleaved tight junctions. *J. Cell Sci.* 13, 763–786.

Takahashi, A., Komiya, E., Kakutani, H., Yoshida, T., Fujii, M., Horiguchi, Y., Mizuguchi, H., Tsutsumi, Y., Tsunoda, S., Koizumi, N., Isoda, K., Yagi, K., Watanabe, Y., Kondoh, M., 2008. Domain mapping of a claudin-4 modulator, the C-terminal region of C-terminal fragment of *Clostridium perfringens* enterotoxin, by site-directed mutagenesis. *Biochem. Pharmacol.* 75, 1639–1648.

Takahashi, A., Saito, Y., Kondoh, M., Matsushita, K., Krug, S.M., Suzuki, H., Tsujino, H., Li, X., Aoyama, H., Matsuhisa, K., Uno, T., Fromm, M., Hamakubo, T., Yagi, K., 2012. Creation and biochemical analysis of a broad-specific claudin binder. *Biomaterials* 33, 3464–3474.

Tsukita, S., Yamazaki, Y., Katsuno, T., Tamura, A., Tsukita, S., 2008. Tight junction-based epithelial microenvironment and cell proliferation. *Oncogene* 27, 6930–6938.

Turksen, K., Troy, T.C., 2011. Junctions gone bad: claudins and loss of the barrier in cancer. *Biochim. Biophys. Acta* 1816, 73–79.

Vermeer, P.D., Einwalter, L.A., Moninger, T.O., Rokhlina, T., Kern, J.A., Zabner, J., Welsh, M.J., 2003. Segregation of receptor and ligand regulates activation of epithelial growth factor receptor. *Nature* 422, 322–326.

Veshnyakova, A., Piontek, J., Protze, J., Waziri, N., Heise, I., Krause, G., 2012. Mechanism of *Clostridium perfringens* enterotoxin interaction with claudin-3/4 protein suggests structural modifications of the toxin to target specific claudins. *J. Biol. Chem.* 287, 1698–1708.

Wodarz, A., Nathke, I., 2007. Cell polarity in development and cancer. *Nat. Cell Biol.* 9, 1016–1024.

Yewale, C., Baradia, D., Vhora, I., Misra, A., 2013. Proteins: emerging carrier for delivery of cancer therapeutics. *Expert Opin. Drug Deliv.* 10, 1429–1448.

Zouhairi, M., Charabaty, A., Pishvaian, M.J., 2011. Molecularly targeted therapy for metastatic colon cancer: proven treatments and promising new agents. *Gastrointest. Cancer Res.* 4, 15–21.

361
362
363
364
365
366
367
368
369
370
371
372
373
374
375
376
377
378
379
380
381
382
383
384
385
386
387
388
389
390
391
392
393
394
395
396
397
398
399
400
401
402
403
404
405
406
407
408
409
410
411
412
413
414
415

